# Evaluation of parameters governing dark and photorepair in UVC-irradiated Escherichia coli

| Journal: | *Environmental Science: Water Research & Technology* |
|---|---|
| Manuscript ID | EW-ART-09-2021-000644.R1 |
| Article Type: | Paper |
| | |

This work identifies key parameters previously overlooked by researchers aiming to understand the potential for bacterial repair after germicidal UV disinfection. Results here show that current models do not adequately account for variable environmental conditions, such as reactivation light intensity and dissolved organic matter, or novel dosing wavelengths.

1    Title: Evaluation of parameters governing dark and photorepair in UVC-irradiated

2                                    *Escherichia coli*

3    Authors:

4     Mostafa Maghsoodi[1], Grace L. Lowry[1], Ian M. Smith[1], Samuel D. Snow[1*]


5    [1]Department of Civil and Environmental Engineering, Louisiana State University, 3255 Patrick
6    Taylor Hall, Baton Rouge, Louisiana 70803, United States.

7    *Corresponding author: ssnow@lsu.edu;

8

9    Abstract:

10   After decades of UV disinfection practice and numerous studies on the potential for pathogens

11   to undergo dark or photo-repair after UV exposure, recent advances in UV light emitting diode

12   (LED) technologies prompt renewed attention to bacterial reactivation and regrowth processes

13   after UV exposure. The aspect of photorepair conditions warrants particular attention, because

14   even studies on conventional mercury vapor lamps have not sufficiently characterized these

15   parameters. Wastewater encounters a wide range of environmental conditions upon discharge

16   (e.g., solar irradiation and dissolved organics) which may affect repair processes and ultimately

17   lead to overestimations of pathogen removal. *Escherichia coli* was used here to investigate the

18   impacts of changing reactivation conditions after $UV_{254}$ and $UV_{278}$ irradiation. $UV_{254}$ and $UV_{278}$

19   doses of $13.75\pm0.4$ mJ·cm$^{-2}$ and $28.3\pm0.8$ mJ·cm$^{-2}$ were required to induce a 3.0-log inactivation

20   of *E. coli*, respectively. Specifically, photoreactivation conditions were varied across dissolved

21   organic matter (DOM) content and photoreactivation wavelengths and intensities.

22   Photoreactivation achieved higher log recoveries than dark repair, ranging from 0.8 to 1.8 log

23   differences, but a secondary disinfection effect occurred under UVA irradiation. During

24   photoreactivation, humic acid inhibited the initial repair of $UV_{278}$-dosed *E. coli* but culture

25   media enhanced recovery for both dosage wavelengths. Photoreactivation profiles under $UV_{395}$,

26     $UV_{365}$, and visible light depended on both fluence and time, with more regrowth observed upon

27     exposure to visible light and the least under 365 nm. The susceptibility of *E. coli* to UVA was

28     increased by prior exposure to UVC.

29

30     Keywords:

31     UV Disinfection; bacteria; photoreactivation; photorepair; regrowth; UV LEDs

32

## 33     1. Introduction

34     Across the globe, microbial contaminants in wastewater discharges threaten public health with

35     water-borne diseases.(1, 2) For this reason, it is essential that disinfection technologies in water

36     treatment systems effectively inactivate pathogens. Conventional ultraviolet (UV) dosing

37     systems are known to be effective at inactivating pathogens via DNA damage,(3) yet there is

38     an important caveat: the potential for cellular repair mechanisms to reactivate UV-dosed

39     organisms.(3, 4) Currently, nearly all germicidal UV (or UVC, 200 to 280 nm) driven

40     inactivation processes use either low pressure mercury lamps with a nearly monochromatic

41     emission at 254 nm or medium pressure lamps with a polychromatic emission.(5, 6) Recent

42     innovations in LED technologies will make it possible to replace mercury lamps with LED

43     counterparts in many UV dosing applications.(5, 7) UV LEDs will ultimately offer several

44     improvements over Hg lamps; for example, UV LEDs provide the ability to optimize

45     wavelengths, reduce light attenuation (via redshifted wavelengths and innovative contactor

46     designs), reduce operational costs, and have longer life expectancies.(8) As challenges of

47     production cost and power output are resolved, UVC LEDs are expected to transform the UV

48     disinfection industry.(9, 10) It is anticipated that UV LEDs will follow the same cost and

49     efficiency trajectory that was observed for other type of LEDs. As an example, the wall plug

50     efficiencies (the optical power output divided by the electrical input power) of blue and red

51   LEDs were increased 80% and 60% respectively in 2010.(11) The American National

52   Standards Institute (ANSI) revised its rule for ultraviolet microbiological water treatment

53   systems (55-2019) in November 2019 to include germicidal LEDs in its guidance.(12)

54       Despite the damage caused by UV irradiation, many microorganisms can counteract the

55   defects with repair mechanisms.(13) Bacteria have two cellular repair modes: dark repair and

56   photoreactivation. Dark repair occurs in the absence of light and replaces damaged DNA sites

57   with undamaged nucleotides via two pathways: base excision repair and nucleotide excision

58   repair.(14) Dark repair mechanisms are controlled by the expression of the recA gene which

59   regulates the induction of over 20 genes.(15) The recA protein plays both  direct  and indirect

60   roles in recombinational repair and controls the induction of the SOS repair genes through its

61   protease function.(16) The dark process is only able to remove thymine dimers when glucose

62   is present.(17) Photoreactivation is a process by which bacteria or bacteriophages (via host

63   cells) can recover from induced UV damage upon exposure to visible or UVA (~320 to 400

64   nm) light.(18, 19) In this process, the pyrimidine dimer photoproducts created by UVC or UVB

65   exposure are repaired by photoactivated enzymes.(19, 20) Photolyase is the biomolecule

66   primarily responsible for the photoreactivation process, containing monomeric proteins of 450-

67   550 amino acids and two non-covalently bound chromophore cofactors.(21) Photolyase is

68   activated by the energy of photons with wavelengths from 330 to 480 nm,(22) binds to

69   cyclobutane pyrimidine dimers (CPDs) or pyrimidine-pyrimidone photoproducts (6-4 PPs), and

70   initiates cycloreversion of the cyclobutane ring, mitigating the adverse effect of UV

71   irradiation.(22)

72   Several predictive models have been put forward since the discovery of photoreactivation with

73   the aim to better understand the fate of UVC-dosed bacteria in environmental systems.(23-25)

74   Building from early models, Nebot Sanz et al. (2007) incorporated an induction period, a lag

75   interval between initial reactivation light exposure and observed reactivation, and accurately

76    matched their experimental data. In Nebot Sanz's model, the data for photoreactivation were

77    obtained across several experimental dimensions, including microbe type, reactivation light

78    exposure, and dark repair time, but their work only considered a low dose of reactivation light

79    ($0.1$ mW/cm$^2$ of UV$_{360}$ for 4 h), well below typical solar intensities (monthly average of $1.0$

80    mW/cm$^2$ for hourly solar radiation in the range of 290 nm to 385 nm).(26) This model was later

81    revised in 2012 by Velez-Colmenares and coworkers by considering the effects of sunlight

82    during reactivation, introducing a first order decay term to their predictive model for cell

83    survivability.(27) In 2017, Li et al. published another adaptation of the Nebot Sanz 2007 model

84    when comparing inactivation by UV LEDs and mercury lamps; their study also used a low

85    photoreactivation dose of $0.12$ mW/cm$^2$ over 8 h. In all these reports, none considered the

86    reactivation light intensity as a variable; most studies examined photorepair on the basis of

87    irradiation time, not fluence.

88    Bacterial repair dynamics may be influenced by the type of damage inflicted, so it is important

89    to determine whether novel UVC dosing wavelengths cause differential repair outcomes.

90    Photoinduced cellular damage can occur in a variety of ways. UVC photons can directly

91    photolyze protein chromophores and cause generalized oxidative stress.(28) Similarly, UVB

92    can cause direct or indirect (via production of endogenous reactive oxygen species) damage to

93    cellular components.(29) The predominant mechanism of UVC inactivation of microorganisms

94    is by causing specific damage to DNA or RNA.(30) In this process the light causes two

95    predominant types of lesions in the genetic code: CPDs and 6-4 PPs.(19, 31) Other nucleic acid

96    photoproducts, such as Dewar isomers, pyrimidine hydrate, thymine glycols, and dipurine

97    adducts, are also produced in smaller amounts during UV irradiation.(13, 14) The type of

98    damage induced depends, in part, on wavelength; for example, in the UVC range (200 to 280

99    nm) the predominant lesions are CPDs and 6-4 PPs and in the UVB range (280 to 320 nm) the

100   formation of Dewar isomers is more efficient and sometimes they are the second most frequent

101    photoproducts after CPDs.(14, 32) In this way, adapting a $UV_{254}$ dosing system to a $UV_{278}$ source

102    may change the nature of the damage microorganisms receive.

103    When wastewater effluent discharges into natural waters, the presence of dissolved organic

104    matter (DOM) and the average incident solar irradiation, about 5% of which is in the UV

105    spectrum,(33) become important considerations. DOM can impact the activity of microbes by

106    directly providing substrate (assimilable organic carbon) for regrowth after repair,(34) by

107    promoting the uptake of nutrients, or—in some cases—by inhibiting growth via toxic

108    effects.(35) The impact of DOM on recovery processes after UVC exposure, however, is not

109    well understood. Likewise, upon mixing with a receiving water, irradiated microorganisms

110    from an effluent discharge will be transported to different positions in the water column and

111    receive differing amounts of solar irradiation. At present, few data are available on

112    photoreactivation under variable reactivation light conditions.

113    In this work, the implications of variable reactivation conditions are explored in the context of

114    using different germicidal wavelengths for *E. coli* disinfection. The extent and kinetics of

115    reactivation are assessed during dark- and photorepair across DOM types and quantities.

116    Photoreactivation profiles for different reactivation light intensities and wavelengths are

117    analyzed on fluence and time bases.

118    **2.    Materials and methods**

119        **2.1. Chemicals**

120    Humic acid and Potassium trioxalatoferrate (III) trihydrate were obtained from Alfa Aesar

121    (Haverhill, MA). 1,10-Phenanthroline, sodium acetate anhydrous, sulfuric acid, Tryptone,

122    Yeast Extract, Dextrose, NaCl, $CaCl_2$, $MgSO_4$ and Phosphate Buffered Saline (PBS) were

123    obtained from VWR (Radnor, PA). Ultrapure water (>18.2 MΩ-cm) from a Nanopure Infinity

124    system (Thermo Fisher Scientific Inc., Waltham, MA) was used.

125    **2.2. Culturing and Enumeration**

126    *E. coli* was used in this work because *E. coli* has been used as an indicator microbe for

127    confirming the presence of pathogens.(36) *E. coli* (ATCC® 15597™) was obtained from

128    American Type Culture Collection (ATCC, Manassas, VA). To enumerate *E. coli*, samples

129    were serially diluted, and the concentration of each sample was measured via a spread plate

130    colony counting technique. In this technique, a sample aliquot was spread on nutrient agar plates

131    then incubated at 37°C for 24 h. Agar plates and culture broth (CB) media contained tryptone,

132    yeast extract, dextrose, NaCl, CaCl$_2$, and MgSO$_4$.(37) *E. coli* sample processing was performed

133    in phosphate buffered saline (PBS) containing 137 mM NaCl, 2.7 mM KCl, and 9.5 mM

134    Phosphate buffer with the resulting pH between 6.6 to 7.2. All samples were measured with at

135    least three plates per sample point and experiments were performed in at least triplicate; error

136    bars represent the standard error of these measurements.

137    **2.3. Irradiance Measurement**

138    The irradiances of each light source were measured by BLUE-Wave UVNb-25 Spectrometer

139    (StellarNet Inc., Tampa, FL). The lamp emission spectra were also recorded. The Bolton and

140    Linden (2003) method was used to calculate UV fluences with the units of mJ·cm$^{-2}$ to account

141    for water, Petri, reflectance, divergence, and attenuation factors.(38) These calculations treated

142    the LEDs to be monochromatic for the purpose of reporting irradiance, since the spectrometer

143    provided a wavelength-integrated measurement. To complement the radiometric fluence

144    calculations, chemical actinometry experiments were performed to measure the intensity of

145    light in units of einstein/min. Potassium trioxalatoferrate (III) trihydrate was used as an

146    actinometer. All the actinometric experiments were performed in a dark room to eliminate the

147    effect of the ambient light. Samples containing potassium trioxalatoferrate (III) trihydrate,

148    sodium acetate and sulfuric acid were irradiated with different light sources and were then

149    mixed with 2 ml of 0.2% aqueous solution of 1,10-phenanthroline and after diluting the mixture

150    with DI water to 10 ml, the absorbance of samples was measured at 510 nm.(39) Equation (1)

151    was used to calculate the light intensity (I):

152    $I = \frac{AV_2V_3}{\varepsilon d\varnothing_\lambda tV_1}$      (1),

153    where the unit for intensity is einsteins/min. $V_1$, $V_2$, and $V_3$ correspond to the volume of the

154    sample taken from the batch, the total volume of actinometer solution, and the dilution volume,

155    respectively, $t$ is the irradiation time, and $d$ is the cell path length used to measure absorption

156    (A). An extinction coefficient ($\varepsilon$) value of $1.11 \times 10^4$ L mol$^{-1}$·cm$^{-1}$ for the ferrous 1,10-

157    phenanthroline complex was used based on Halchard and Parker's work, and quantum yield

158    values at given wavelengths ($\phi_\lambda$) of ferrous production were obtained from a previous

159    report.(39)

**2.4. UV Inactivation**

161    Inactivation experiments were performed by exposing *E. coli* to UV light from several sources.

162    A UV LED (LG Innotek UVC 6868, South Korea) with an emission peak at 278 nm (UV$_{278}$,

163    11.5 nm FWHM) was used, and quasi-collimated irradiation was achieved by situating the LED

164    above a black tube with the sample below; a schematic of this cabinet is shown in Figure S1 of

165    the Supporting Information (SI). Separately, a 15 W low pressure mercury lamp (Sankyo Denki

166    Co., Japan) with an emission peak at 254 nm (UV$_{254}$, 4.0 nm FWHM) was used. All emission

167    spectra from light sources used for their germicidal effects are illustrated in Figure 1. All

168    inactivation experiments were conducted inside an enclosed photoreactor cabinet equipped with

169    a magnetic stirrer and kept at room temperature via cooling fans. The distance between samples

170    and UV light source was adjusted to 20 cm which provided intensity values of 371 µW·cm$^{-2}$ for

171    the Hg lamp and 722 µW·cm$^{-2}$ for the UV LED.

172
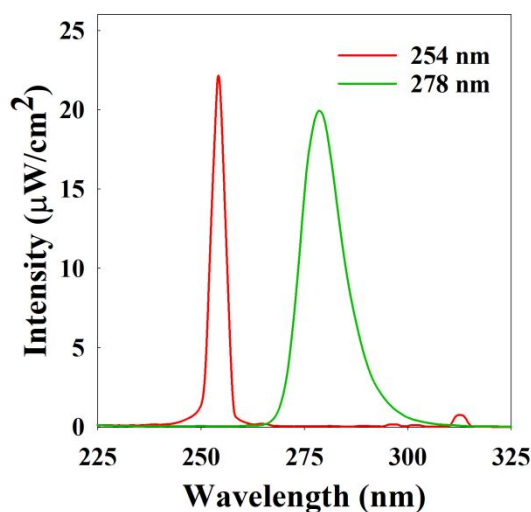


**Figure 1.** Emission spectra from UVC lamps used for disinfection.

173    UV dosing was performed in a sterilized glass Petri dish with a 5 cm diameter and a depth of

174    1.5 cm; *E. coli* was diluted by adding PBS to reach a reactor volume of 10 mL. The resulting

175    concentration was $10^7$ CFU·mL$^{-1}$ for *E. coli*. DOM experiments were performed using either 25

176    mg·L$^{-1}$ humic acid (HA) or CB at a dextrose concentration of 25 mg·L$^{-1}$. The absorbance of

177    each sample was measured in a 1 cm quartz cuvette using a UV-Vis spectrophotometer

178    (UV3100-PC, VWR, USA).

179    **2.5. Repair Experiments**

180    Repair experiments were conducted for 9 h periods under dark or irradiated conditions after

181    imposing at least a 3.0-log inactivation to be consistent with similar, recent work.(36) In these

182    cases, $N_o$ was defined as the number of viable cells per volume in solution prior to disinfection;

183    $N_d$ was used to designate the viable cells at the end of disinfection and the beginning of repair;

184    and N denotes the concentration at a given time. Sample aliquots were taken at intervals, serially

185    diluted, and plated immediately thereafter. In dark repair experiments, samples were kept in a

186    clean dark chamber for 9 h. Five different light conditions including UVA lights with emission

187    peaks at 365 and 395 nm and a visible light (see Figure 2 for obtained emission spectra) were

188       used  to  investigate  fluence  and  wavelength  effects  on  the  photoreactivation  process;
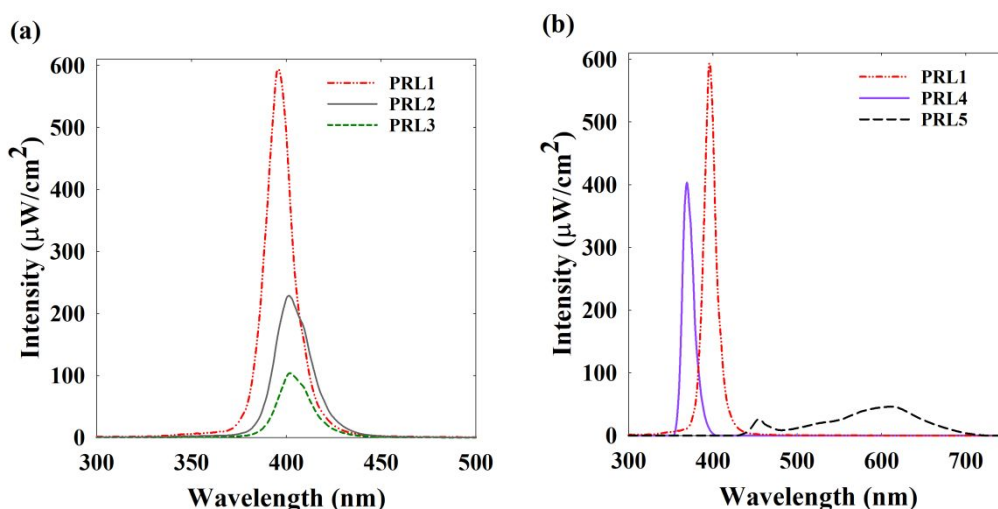


**Figure 2.** Emission spectra of lamps used for experiments with variable photoreactivation (a) intensities and (b) wavelengths.

189       abbreviations, emission parameters, and manufacturer information are provided in Table 1.

190       PRL refers to photoreactivation lamp and the numbers are arbitrarily assigned such that PRLs

191       1-3  are  $UV_{395}$  lamps  of  differing  intensities,  PRL4  is  a  $UV_{365}$  lamp,  and  PRL5  is  a

192       polychromatic white lamp. The majority of the photoreactivation experiments were conducted

193       using PRL1. The effects of irradiation dosages on photoreactivation were assessed using three

194       LED arrangements with emissions centered at 395 nm: PRL1, PRL2, and PRL3. The effects of

195       wavelength on photoreactivation were investigated using three lamps: PRL1, PRL4, and PRL5.

196       The visible light case (PRL5) adds a case relevant to conditions with limited UV light, such as

197       indoor storage of UV-treated drinking water. The effects of DOM on the repair processes were

198       assessed by adding 25 mg·L$^{-1}$ of DOM (either HA or CB) to the reaction mixture prior to the

199       UV inactivation step. Data are presented primarily as normalized log values ($\log[N/N_d]$) to

200       compare the repair of different experiments on a basis of relative recoveries. The slopes of the

201       decay portion of photoreactivation experiments were compared via a t-test to determine if the

202       difference  in  the  results  of  experiments  is  significant  ($p < 0.05$). Survival  fractions  ($S_t$,

203       $N/N_o*100$) are used when evaluating predictive models.

9

204          **Table 1.** Actinometry data for light sources used in photoreactivation experiments.

| Abbreviation | Light intensity (einsteins/min) | Emission peak (nm) | LED manufacturer | FWHM (nm) |
|---|---|---|---|---|
| **PRL1** | $8.04 \times 10^{-5}$ | 395 | LG Innotek Co., 6868 | 15.5 |
| **PRL2** | $2.19 \times 10^{-5}$ | 395 | TSLC Corp., C3535U-UNL | 15.5 |
| **PRL3** | $7.33 \times 10^{-6}$ | 395 | TSLC Corp., C3535U-UNL | 15.5 |
| **PRL4** | $9.38 \times 10^{-5}$ | 365 | LG Innotek Co., 6868 | 15.1 |
| **PRL5** | $6.49 \times 10^{-7}$ | Polychromatic, visible 3000K | Brizled Inc., DDL6 | N/A |

205

206      **2.6. Photoreactivation Model and Parameterization**

207      A model put forward by Velez-Colmenares et al. in 2012, which included a decay term was

208      used to fit experimental data and to compare how prior estimations of model parameters map

209      onto present observations. The Velez-Colmenares model (VC model hereafter) shown in

210      Equation 2 was derived to incorporate a photorepair term with a decay term for the germicidal

211      effects of sunlight. In the equation,

212      $$S_t = (S_m \cdot e^{-M_s t}) - (S_m - S_o) \cdot e^{-(k_s + M_s) \cdot t} \qquad (2),$$

213      $S_t$ is survival at time t (min), $S_m$ is the maximum survival ratio, $S_o$ is the initial survival fraction

214      immediately after UVC irradiation, $(S_m - S_o)$ is thus the fraction of microorganisms that can be

215      reactivated with respect to the initial concentration, $M_s$ represents the rate constant for UVA

216      decay (min$^{-1}$), and $k_s$ is the photoreactivation rate constant (min$^{-1}$). Predictive model fits were

217      generated via Microsoft Excel spreadsheets using parameters derived from either the UVC-

218      fluence empirical relationships put forward alongside the VC model or by using the Excel

219      Solver functionality.(27) In the Solver analysis, the squared sum of errors value was minimized

220      for the difference between predicted and observed values while constraining the $M_s$ term to be

221      $\geq$ observed decay rates, discussed below, and the $(S_m - S_o)$ term to be the difference between

222    the solver formulation for $S_m$ and the observed $S_o$ value. $R^2$ values were determined according

223    to the total variance between observed data and model fit.

## 3. Results

### 3.1. *E. coli* inactivation

226    Inactivation profiles of *E. coli* by different wavelengths in the presence and absence of DOM

227    are shown in Figure 3. In the absence of DOM, the UV doses, reported as incident intensities,

228    required to obtain 3.0-log inactivation at 254 nm and 278 nm were found to be 13.75 mJ·cm$^{-2}$

229    and 28.3 mJ·cm$^{-2}$, respectively. The UV$_{254}$ dose requirement of 13.75 mJ·cm$^{-2}$ was similar to

230    the 12 mJ·cm$^{-2}$ in a 2017 study;[40] the UV$_{278}$ dose of 28.3 mJ·cm$^{-2}$, however, was surprising

231    because most reports place the dose requirement for a 3-log reduction near 12 mJ·cm$^{-2}$.[36, 40]

232    The discrepancy here appears to relate to the extended shoulder, observed to extend to about 12

233    mJ·cm$^{-2}$. In the presence of DOM, the required doses for obtaining 3.0-log inactivation, after

234    adjusting for light absorption, did not appear to be significantly different from the non-DOM

235    cases, at 11.6 mJ·cm$^{-2}$ for UV$_{254}$ and 26.6 mJ·cm$^{-2}$ for UV$_{278}$. At higher concentrations (50 mg·L$^{-1}$

236    $^{1}$), humic substances have been shown to provide localized UV shielding for bacteria, beyond

237    attenuation in the bulk phase.[41] The 25 mg·L$^{-1}$ used here did not appear to significantly affect

238    the disinfection process.
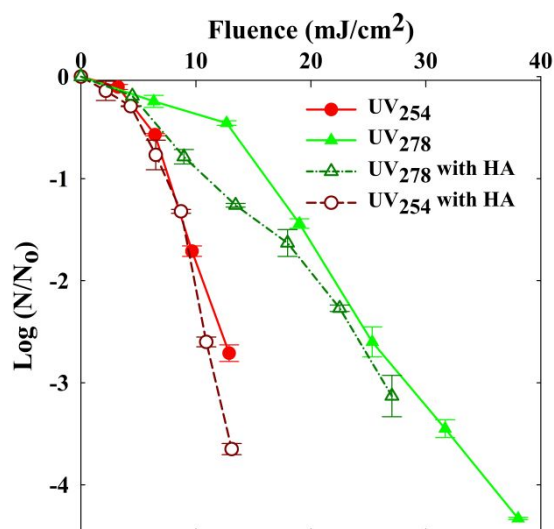
**Figure 3.** Inactivation of *E. coli* with 25 mg·L$^{-1}$ HA or in PBS alone by UV$_{254}$ and UV$_{278}$.

239

240    **3.2. Dark repair of *E. coli***

241    Dark repair experiments were conducted using bacteria inactivated by UV$_{254}$ or UV$_{278}$, with

242    results plotted in Figure 4. A reference line shows the typical growth kinetics of *E. coli* over 9

243    h in the dark; the trendline was calculated from experiments shown in Figure S2 in which *E.*

244    *coli* was diluted by 3-log, in place of disinfection, then provided HA, CB, or just PBS. After 9

245    h, *E. coli* recovered 1.3 and 1.1 logs after UV$_{254}$ or UV$_{278}$ exposure, respectively. These values

246    fell well below the growth of *E. coli* that were not subject to UVC dosing, but the initial

247    recovery of cells exposed to UV$_{278}$ was more rapid than growth alone, when DOM was

248    available. The presence of a carbon source, HA or CB, allowed UV$_{278}$-exposed cells to repair

249    faster than all other cases. Here, dark repair rates, between 0.5 and 1.6 logs, outpaced total dark

250    recoveries reported by Nyangaresi et al. (2018), which were at most 0.24 logs for several

251    disinfection wavelengths. Given the minimal difference between irradiation sources with peaks

252    at 275 and 278 nm and that both studies accounted for inactivation on a fluence basis, the

253    difference in recoveries is likely a result of differing solution conditions: Nyangaresi et al. used

254    deionized water for all their experiments while PBS was used here to avoid cell death via

255    osmotic shock.
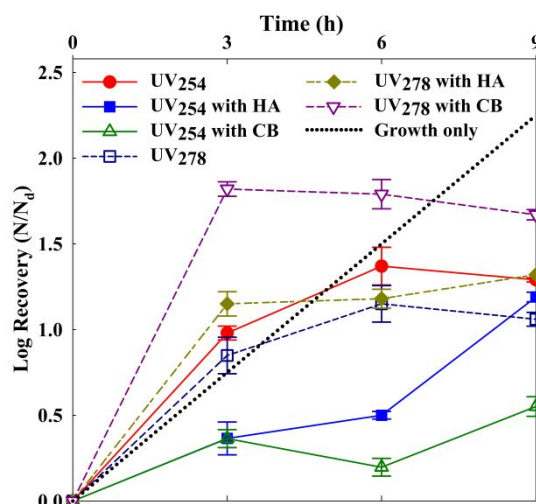
**Figure 4.** Dark repair of $UV_{254}$- or $UV_{278}$-dosed *E. coli* with 25 mg·$L^{-1}$ HA, 25 mg·$L^{-1}$ CB, or in PBS only. The black dotted line (••••) represents the growth of *E. coli* after dilution, in place of UV exposure, to the same initial concentration

256

257    The effects of DOM on dark repair were investigated by adding HA or CB to the reaction

258    solutions. HA has been shown to behave as a growth regulator for some bacteria and may affect

259    cellular repair processes.(42) Most dark repair observations here matched the profile of the

260    reactivation model put forward by Nebot Sanz et al. (2007) with an induction period, growth

261    phase, stabilization phase and decay period. HA inhibited the recovery of $UV_{254}$-dosed *E. coli*

262    in the first 6 h, but the rate increased between 6 and 9 h such that the log recovery with HA at

263    9 h was similar with or without HA. The recovery was higher in the absence of HA for the first

264    6 h of dark repair after $UV_{254}$ exposure than with HA; this trend was not observed in the dark

265    repair profile of $UV_{278}$-dosed *E. coli*. CB was used to provide *E. coli* with favorable growth

266    conditions, in order to investigate the effect of nutrients on the dark repair. Although more

267    recovery was expected with CB because of the availability of glucose, a highly efficient carbon

268    and energy source for *E. coli*,(43) fewer $UV_{254}$-dosed bacteria recovered in the presence of CB

269    than without any DOM. After $UV_{278}$-dosing, however, more repair was observed with added

270    CB than without. CPD and 6-4 PP are formed at higher rates during irradiation by $UV_{254}$ than

271    by $UV_{278}$,(44) whereas red-shifted wavelengths have been found to promote more oxidative

272    stress.(45) Given that photolyase functions specifically to repair nucleic acid dimerizations, it

13

273     is likely that the oxidative damage is more difficult for bacteria to repair.

274     **3.3. Photoreactivation of *E. coli***
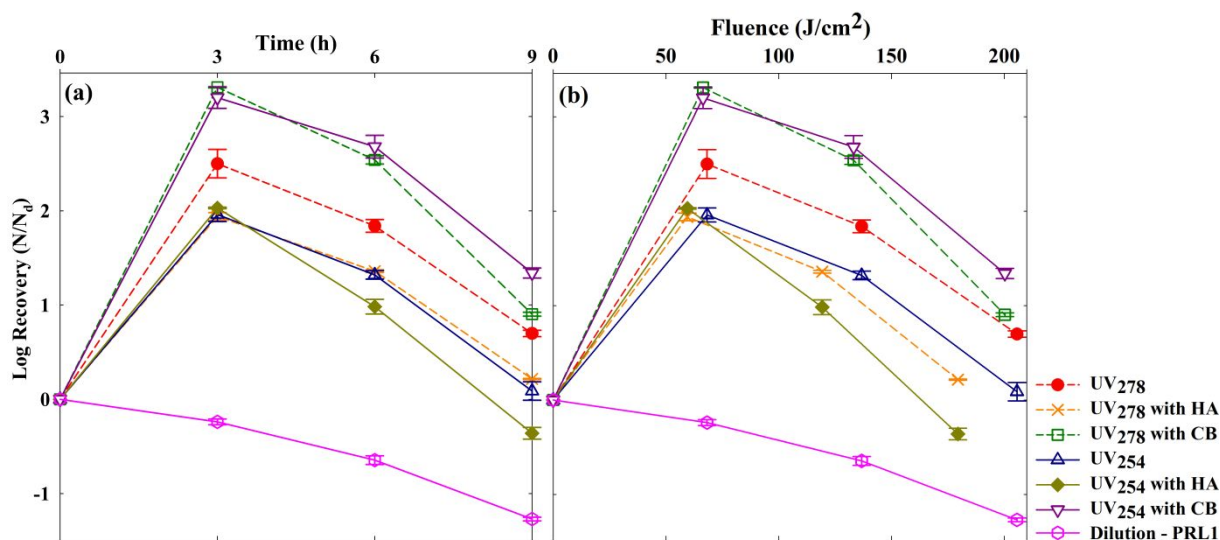


**Figure 5.** Photoreactivation of *E. coli* using PRL1 in the presence or absence of 25 mg·L$^{-1}$ of HA or CB after inactivation by UV$_{254}$ and UV$_{278}$. Data are displayed on the bases of (a) time and (b) fluence. A reference of *E. coli* inactivation under PRL1 with no prior UVC-dosing is also shown (—⊖—).

275     The photoreactivation of *E. coli* after different UVC sources was studied using PRL1 (with an

276     emission peak at 395 nm) as the reactivation light source. The results of these experiments are

277     illustrated in Figure 5. All cases showed higher recoveries, during the repair phase, than the

278     portion of cells restored during the dark repair. The maximum log recoveries of the dark- and

279     photorepair experiments are shown in Table 2. During the repair phase and in the absence of

280     DOM, recovery of UV$_{254}$-dosed *E. coli* was lower than that of the UV$_{278}$-dosing case. Net log

281     recoveries were also calculated for the first 3 h of photorepair by taking the difference of the

282     photorepair case and the observed decay of diluted *E. coli* under PRL1 which were not exposed

283     to UVC; these values are shown in Table 3. The presence of CB increased the rate of photorepair

284     after exposure to both wavelengths. Conversely, the addition of HA inhibited the initial

285     photorepair after UV$_{278}$-dosing but did not change the UV$_{254}$-dosing case. After 3 h a decay

286     phase was observed under PRL1, where UVA damage caused cell viability to decline. UVA is

287     known to affect bacterial survivability by several mechanisms, including membrane

288     damage,[46] photo-induced oxidative stress,[47-49] and decreased metabolic activity.[50] The

289    decay rate constants for the experiments were estimated by linear regression from 3 h to 9 h, as

290    shown in Figure S3 and recorded in Table S1. Rates were not observed to be meaningfully

291    different when compared across dosing wavelengths or DOM conditions. Notably, a correlation

292    generated for all cases of decay post-photorepair (see Figure S3(b)), was different ($p < 0.05$)

293    from the case where *E. coli* was exposed to UVA without prior UVC exposure. The non-repair

294    case had a decay constant of 0.17 h$^{-1}$, while the collective decay constant for the photorepair

295    cases was 0.33 h$^{-1}$. Despite the initial photoreactivation effect, *E. coli* were more susceptible to

296    UVA irradiation after UVC-dosing.

297    **Table 2.** The mean and standard error recoveries ($\log[N/N_d]$) in the initial 3 h after UVC
298    inactivation and for dark- and photorepair experiments.

| Conditions | UV$_{254}$-dosed | | UV$_{278}$-dosed | |
|---|---|---|---|---|
| | Dark Repair | Photoreactivation | Dark Repair | Photoreactivation |
| **Without DOM** | $0.98 \pm 0.04$ | $1.96 \pm 0.07$ | $0.85 \pm 0.1$ | $2.50 \pm 0.15$ |
| **With HA** | $0.37 \pm 0.09$ | $2.03 \pm 0.01$ | $1.15 \pm 0.07$ | $1.94 \pm 0.04$ |
| **With CB** | $0.36 \pm 0.05$ | $3.20 \pm 0.11$ | $1.82 \pm 0.04$ | $3.13 \pm 0.01$ |

299

300    The photoreactivation profiles for all PRL1 cases comprised a repair phase in first 3 h followed

301    by a decay period thereafter. This trend differed from photoreactivation described by Nebot

302    Sanz et al. (2007) and Nyangaresi et al. (2018), which entailed growth, stationary, and mortality

303    phases.(36, 51) While their models used a zeroth order decay constant for bacteria mortality, a

304    first order decay was observed in the present study, induced by more intense UVA irradiation.

305    The photoreactivation profiles observed here more closely match a model developed to predict

306    solar reactivation of wastewater discharges, which incorporated a first order decay term.(27)

307    The differences between models highlight the importance of reporting reactivation fluences and

308    the consideration of the context where photorepair may occur. Figure 5(b) plots recoveries

309    under PRL1 by fluence. The highest recovery observed occurred at ~65 J/cm$^2$, a value much

310    higher than an estimated 1.44 J/cm$^2$ in the report by Nebot Sanz et al., based on their reported

311    conditions of 4 h of 0.1 mW/cm$^2$ UVA. PRL1 provides a reasonable representation of intense

312    solar light, since typical solar UVA irradiance values reach upwards of 5.0 mW/cm$^2$, which

313    corresponds to 162 J/cm$^2$ over 9 h.(52)

314    **Table 3.** Repair (log[$N/N_d$]) during initial 3 h of photoreactivation after $UV_{254}$- or $UV_{278}$-
315    dosing, adjusted for observed growth or decay observations without UVC exposure. Error
316    values represent standard error.

| Reactivation Condition | Log repair ($UV_{254}$-dosed) | Log repair ($UV_{278}$-dosed) |
|---|---|---|
| PRL1 | $2.20 \pm 0.03$ | $2.74 \pm 0.05$ |
| PRL1 + HA | $2.27 \pm 0.01$ | $2.18 \pm 0.02$ |
| PRL1 + CB | $3.44 \pm 0.04$ | $3.37 \pm 0.01$ |
| PRL2 | $1.65 \pm 0.01$ | $2.30 \pm 0.04$ |
| PRL3 | $1.36 \pm 0.05$ | $1.40 \pm 0.04$ |
| PRL4 | $2.26 \pm 0.07$ | $2.16 \pm 0.06$ |
| PRL5 | $1.82 \pm 0.07$ | $2.27 \pm 0.03$ |

317

318    *3.3.1. Effects of Photoreactivation Light Intensity*

319    Given the importance of reactivation light dose, experiments were performed using three

320    different intensities to disambiguate the roles of reactivation time and dose on the photorepair

321    process. Three $UV_{395}$ light sources were used to test the effects of photoreactivation intensities

322    on the photorepair process: PRL1 providing the highest intensity, followed by PRL2, then

323    PRL3. The spectra for the light sources are shown in Figure 2(a). Data from photoreactivation

324    experiments with these light conditions are displayed in Figure 6. After inactivation with $UV_{278}$

325    light, bacteria recovered at the same rate for PRL1 and PRL2 in the first 3 h, but the decay for

326    PRL2 was much slower than that for PRL1. The repair phase for recovery under PRL2 lasted

327    for just 3 h after $UV_{278}$-dosing, but after $UV_{254}$-dosing it lasted for 6 h. Reactivation under

328    PRL3, the least intense lamp, yielded recovery that extended to 6 h for the $UV_{278}$-dosed bacteria

329    and through 9 h for the $UV_{254}$ case. The log repair maxima under PRL2 and PRL3 were similar,

330    and both were lower than the PRL1 recovery. The UVA reactivation dose was important

331    because UVA is only sublethal up to about 40 J/cm$^2$ for stationary phase bacteria.(53, 54) After

332    this point, cellular repair and protection processes may have been overwhelmed by the stress of

333    the incident light. For example, UVA-sensitive chromophores within bacterial cells can cause

334    thiouridine crosslinking, leading to depressed protein synthesis.(54)
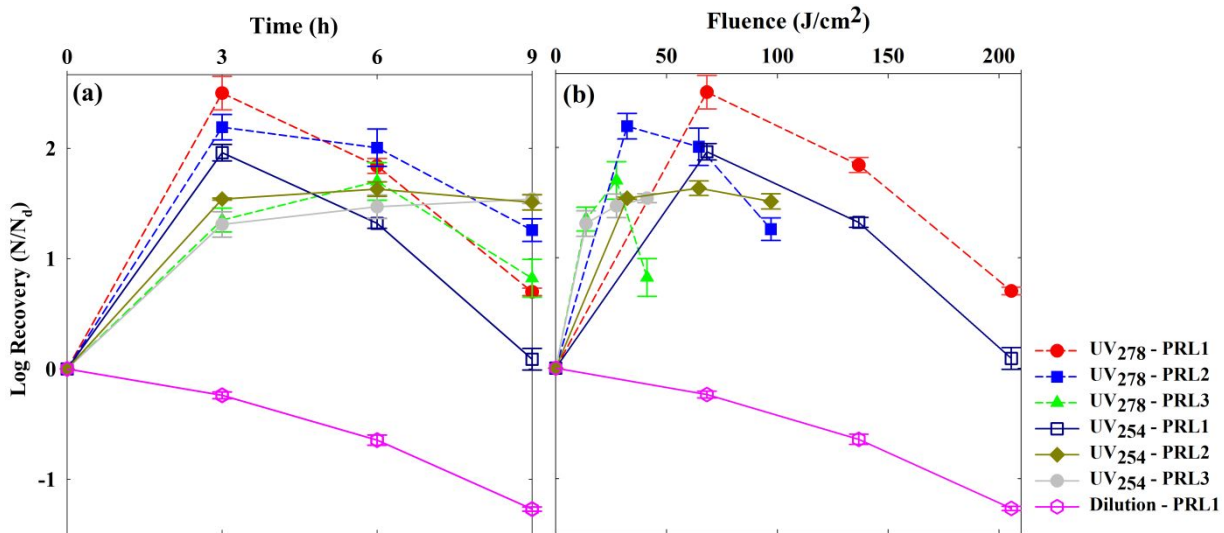


**Figure 6.** Photoreactivation of $UV_{254}$- or $UV_{278}$-dosed *E. coli* under different reactivation light intensities based on (a) time and (b) fluence. A reference of *E. coli* inactivation under PRL1 after dilution instead of UVC-dosing is also shown (—⊖—).

335    Variations in photoreactivation capacities, as measured by the lengths of photorepair phases,

336    are likely affected by two factors: the reactivation dosage received and the type of damage

337    inflicted during disinfection. In 2021 Pousty et al. confirmed that intracellular damage

338    mechanisms depend on UV wavelength and showed that reactive oxygen species can damage

339    DNA or cause general oxidative stress.(45) Photoreactivation trends for the three $UV_{395}$ lamps,

340    each with different intensities, are shown in Figure 6(b). Upon examination of the time and

341    fluence reactivation profiles, one distinction is immediately apparent between $UV_{254}$- and

342    $UV_{278}$-dosed cases. The peak recovery value for $UV_{254}$-dosed *E. coli* was reached at

343    approximately 65 J/cm$^2$ regardless of light intensity (this fluence was only reached for PRL1

344    and PRL2 but PRL3's trend appears to be nearing a plateau before 50 J/cm$^2$). However, $UV_{278}$-

345    dosed *E. coli* were subsequently less resistant to $UV_{395}$ at low light intensities (PRL2 and

346    PRL3). It is likely that oxidative stress introduced by UVA interferes with the photolyase repair

347    pathway; a report by Song et al. in 2019 demonstrated that UVA pretreatment followed by UVC

17

348    dosing prevented subsequent photorepair.(55) From these data, it is clear that the

349    photoreactivation process depends on both time and irradiation intensity; neither fluence- nor

350    time-based calculations provide a complete understanding of the photoreactivation process.

351    This observation demonstrates that at high fluences the reactivation model suggested by

352    Bohrerova and Linden does not predict reactivation, just as they surmised in their analysis,

353    because of a decay term.(56) The VC model provides a similar framework which uses a first

354    order decay constant to account for damage by sunlight. All UVA photorepair experiments,

355    except the $UV_{254}$-PRL2 and -PRL3 cases, appear to have a first order decay period after initial

356    reactivation. The exceptions here would be better fit to a zero-order decay term as suggested by

357    studies using low intensity reactivation lamps.(36, 51) The susceptibility of *E. coli* to $UV_{395}$

358    depended on the wavelength of prior UVC exposure, and the rate of UVA-induced inactivation

359    did not depend on fluence in a linear manner. This difference in cell susceptibilities shows that

360    $UV_{278}$-dosing damaged *E. coli* in a different manner (likely oxidative stress) compared to

361    $UV_{254}$.(45) A simple explanation would be that $UV_{278}$-dosing damages cellular mechanisms

362    that provide UVA resistance. An alternate hypothesis is that *E. coli* can recover more quickly

363    from $UV_{278}$-dosing, leading to a higher repair rate—an observation borne out in nearly all

364    experiments here. Rapid growth rates make bacteria more vulnerable to stressors like heat or

365    UVA,(53) but it is not clear if this principle would apply to regrowth from repair processes in

366    the same manner. Further investigation is needed to identify the mechanisms responsible for

367    the differential behavior of $UV_{254}$- and $UV_{278}$-dosed *E. coli*.

368        *3.3.2. Effects of Photoreactivation Wavelength*

369    Light sources of different wavelengths were applied for the photoreactivation to assess the

370    effects of the photon energy on the photorepair process; emission spectra of these light sources

371    are illustrated in Figure 2(b). The results of photoreactivation under different wavelengths, on

372    a time basis, are shown in Figure 7(a). Photorepair was observed in the first three hours in all

373    cases. In contrast to the other PRLs, photoreactivation under the visible light (PRL5) maintained

374    continued throughout the 9 h, undergoing some growth in addition to repair. The rate of

375    photorepair under exposure of 365 nm light (PRL4), on the other hand, was lower than both

376    PRL1 and PRL5. PRL4 induced the most decay after the recovery phase among all light sources

377    and based on the work of Nelson et al. (2018), $UV_{365}$ causes damage through the production
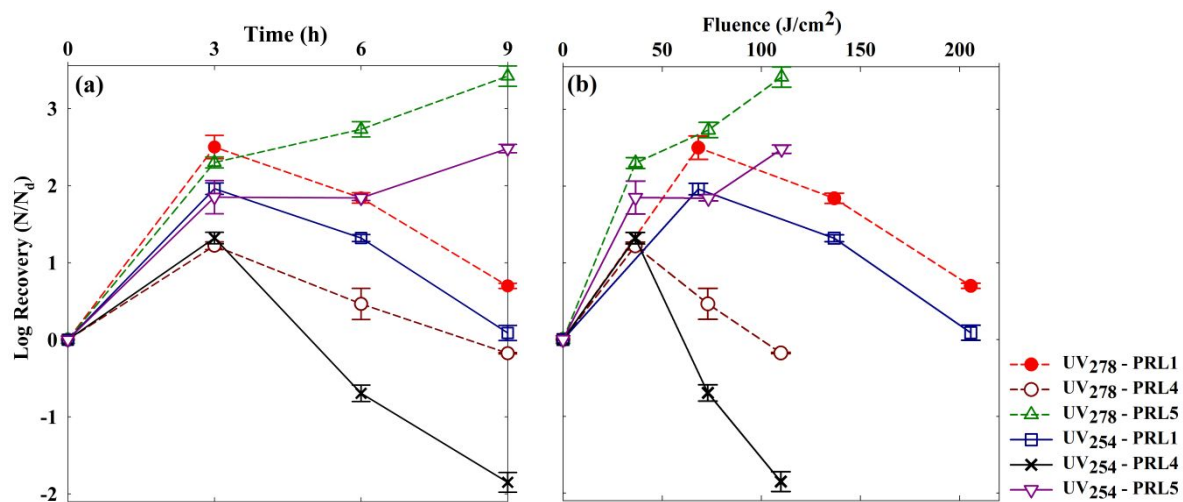


**Figure 7.** Photoreactivation of *E. coli* using different light sources after inactivation with $UV_{254}$ and $UV_{278}$ based on (a) time and (b) fluence.

378    of reactive oxygen species or photochemically produced reactive intermediates,(29) explaining

379    the higher inactivation compared to other PRLs. Inactivation kinetics under these conditions

380    without prior disinfection are shown in Figure S4, and the inactivation values at 3 h were used

381    to calculate the log repair values provided in Table 3. In general, recovery in the $UV_{278}$-dosed

382    cases were higher than the $UV_{254}$-dosed cases. The pattern for photoreactivation with PRL4 was

383    the same as PRL1: a repair phase followed by an inactivation phase.

384    The fluence-basis data for photorepair under various reactivation light spectra are plotted in

385    Figure 7(b). Little difference was observed between the fluence- and time- bases for the

386    disparate lights. Both time-based and fluence-based calculations confirmed that the amount of

387    photoreactivation under visible light was higher than under $UV_{395}$ or $UV_{365}$. Although

388    Bohrerova and Linden reported that there was no significant change in photorepair rate between

389    several visible lamp types (full spectrum lamps (5500K), cool white lamps (2700K), and

390    fluorescent lamps (5500K)),(56) differences between UVA light sources are certainly

391    important, due to lethal effects at high fluences. A cell's ability to perform photorepair depends

392    on three factors: the presence of photolyase in the cell, the number of photons received, and the

393    wavelength of the light.(57) The larger maximum log recoveries found for the visible light cases

394    may be explained by the enzyme's light absorption, which is strongest in the visible range,(19,

395    54) but the situation is complicated by deleterious effects of UVA. The differential effects of

396    photoreactivation wavelengths were described by Jagger (1981), in which he reported that

397    sublethal effects could be observed up to a specific, wavelength-dependent dose limit.

398    Specifically, the sublethal effects were found to begin at about 2 J/cm$^2$ for $UV_{334}$ and 10 J/cm$^2$

399    for $UV_{366}$, reaching lethality at roughly one order of magnitude higher fluence.(58) Sublethal

400    effects might have also contributed to the slowing initial repair in the UVA cases compared to

401    visible, but this effect was small compared to the result of reaching lethal UVA doses. In parallel

402    to the observed trend for the high intensity $UV_{395}$ lamp (PRL1, Figure 6), the decay phase during

403    photoreactivation by $UV_{365}$ was more pronounced after disinfection by $UV_{254}$ than with $UV_{278}$.

404        *3.3.3.  Photoreactivation Model Fitting*

405    The rate constants for reactivation and decay by UVA during photoreactivation were estimated

406    by employing the VC model fitted to experimental data with additional timepoints before 3 h.

407    Figure 8 shows survival fractions $UV_{254}$- or $UV_{278}$-dosed of *E. coli* during photoreactivation

408    under PRL1 compared to predicted trends from either VC model parameter estimations,(27)

409    using 13.75 mJ/cm$^2$ as the $UV_{254}$ fluence value, or based on a non-linear regression of the

410    observed data. Even though the same *E. coli* strain (ATCC 15597) was used in both studies, a

411    direct comparison was not appropriate due to differences in inactivation and photoreactivation

412    light wavelengths and fluences. In their work, Velez-Colmenares and coworkers (2012) derived

413    empirical relationships between several parameters ($S_m$, $k_s$, and $[S_m - S_o]$) and $UV_{254}$ fluence,

414    from 50 to 150 mJ/cm$^2$. While it is not clear that they accounted for light attenuation or other

415    factors within their reactor, the 13.75 mJ/cm$^2$ UV$_{254}$ applied here requires unreasonable

416    extrapolation. The VC model used an M$_s$ value derived from the solar decay of *E. coli*, whereas

417    PRL1 is a high intensity UV$_{395}$ source.(27) For these reasons, it is not surprising that the

418    fluence-based parameter estimates did not fit the UV$_{254}$ observations here. Using a non-linear

419    regression to fit the observed data, however, yielded good fits for both UV$_{254}$ and UV$_{278}$

420    photoreactivation profiles, with R$^2$ coefficients of 0.967 and 0.979, respectively.
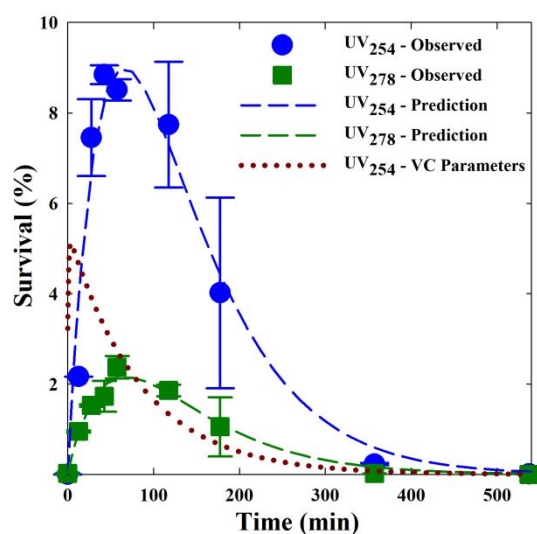


**Figure 8.** Observed survival fractions during photoreactivation of UV$_{254}$- and UV$_{278}$-
dosed *E. coli* with corresponding non-linear fits and a UV$_{254}$ prediction using
parameters from the Velez-Colmenares formulae.

421

422    The estimated and regression-fitted parameters are tabulated in Table 4. The M$_s$ values derived

423    here (0.0136 and 0.0132 min$^{-1}$) were close to 0.0119 min$^{-1}$ used by Velez-Colmenares et al.

424    (2018). These decay constants are significantly larger, however, than the decay rate observed

425    under PRL1 (0.00283 min$^{-1}$) with no prior UVC irradiation, indicating that UVC dosing causes

426    *E. coli* to be more susceptible to subsequent UVA exposure. Differences in S$_m$ and k$_s$ values

427    were most notable compared to the previous report,**(27)** both likely explained by the disparate

428    experimental conditions described above. The fitted parameters, then, provide more reasonable

429    values. Here, a high S$_m$ indicates that many, if not all, of the damaged cells can be repaired after

430    UV$_{254}$ or UV$_{278}$ doses that caused initial 3-log reductions to viability. Conversely, the observed

21

431    $k_s$ values were much smaller than those reported in Velez-Colmenares et al. (2012); the small

432    fraction of repairable bacteria in their work, due to large inactivation doses, inflates $k_s$ compared

433    to cases where the majority of bacteria can undergo photorepair. The peak recoveries observed

434    here occurred between 60 and 75 minutes under PRL1, whereas the 2012 study showed peak

435    reactivation within the first 10 minutes of photorepair.(27) Notably, the $UV_{254}$ dosed bacteria

436    recovered to a much higher fraction than $UV_{278}$ upon examination of data points within the first

437    two hours of reactivation. The slower repair kinetics observed here have significant

438    environmental implications, because fecal coliform monitoring in wastewater effluent will not

439    provide accurate estimates of the discharge's real impact if photorepair causes peak recovery

440    downstream. Considering the DOM (Figure 5) and reactivation wavelength experiments

441    (Figures 6 and 7), it is apparent that the delayed recovery maxima are exacerbated by two

442    factors. First, nutritious DOM increases the effective $S_m$ by allowing growth in addition to

443    repair. Second, variations in reactivation light intensity and wavelength can change $M_s$ and $k_s$.

444    Prediction of the time at which maximum recoveries occur may be as important, if not more so,

445    than the maximum values.

446
447    **Table 4.** Model parameters, calculated or fitted, used in the predictive models for survival in
448    Figure 8, with corresponding $R^2$ values.

| Parameter | Calculated $UV_{254}$[a] | Fitted $UV_{254}$ | Fitted $UV_{278}$ |
|---|---|---|---|
| $S_m$ | 5.41 | 104.7 | 27.5 |
| $M_s$ | 0.0119 | 0.0136 | 0.0132 |
| $k_s$ | 1.03 | 0.00358 | 0.00313 |
| $(S_m - S_o)$ | 2.18 | 104.7 | 27.5 |
| $R^2$ | N/A | 0.967 | 0.979 |

449    [a]Values taken from or calculated according to empirical formulae by Velez-Colmenares et al. (2012).
450

## 4. Conclusions

452    The examination of photoreactivation conditions revealed three important considerations

453    regarding UV disinfection applications. First, according to *E. coli* survival fractions and

454    susceptibilities to low intensity UVA, $UV_{278}$-dosing may yield a net, comparative benefit in

455    inactivation credit for wastewater discharges into waters receiving moderate to low amounts of

456    sunlight. On the other hand, a red-shift in disinfection wavelengths appeared to increase the

457    recovery potential for *E. coli* in the dark, especially in the presence of plentiful nutrients. These

458    contrasting effects reveal a significant need to better understand and model systems where both

459    dark and photorepair processes are expected to occur in tandem (e.g. wastewater discharged to

460    a murky column of water with limited UV light penetration). Second, new challenges to the

461    development of predictive models of photoreactivation were identified. If photoreactivation

462    was dependent solely on the absorption of photons by photolyase, then reactivation fluence

463    would predict the photorepair dynamics. The results here, however, point to the combined

464    relevance of time and light intensity on the repair rate and to the dependence of UVA-induced

465    decay on the reactivation light intensity and wavelength. Further study is required to establish

466    empirical relationships between these factors and their corresponding model parameters (i.e.,

467    $M_s$ and $k_s$). In addition to the influence of reactivation parameters, the results here also point to

468    a need for improved parameterization on the UVC dosing side of the system.

469    Finally, established empirical relationships for model parameters were unable to predict

470    observations here, despite using the same *E. coli* strain and $UV_{254}$. The VC model and the

471    associated parameterizations were based on pilot dosing systems which undoubtedly functioned

472    as a non-ideal reactor,(27) whereas the present study—like many others—used small batch

473    reactors to approximate ideal mixing conditions. This difference evokes an important question

474    of how to properly account for a distribution of dosages which will inevitably result in non-

475    ideal reactor conditions when predicting reactivation profiles. There is a critical need to define

476    and measure UV dosing in terms of fluence experienced by the treated water rather than on the

477    basis of lamp outputs. The translation of laboratory studies to full scale treatment facilities is

478    vital but currently insufficient; future models should incorporate a distribution of UV-dosages

479    received by bacteria as occurs in non-ideal systems. Some regulatory estimations exist for

480    accounting for the repair of bacteria in wastewater effluent and operational conditions can be

481    adjusted to mitigate photorepair,(59) but these efforts are currently rudimentary in nature and

482    require improvements in order to effectively account for variable conditions and novel

483    disinfection wavelengths. Current predictive models and their parameterization must be

484    improved to empower regulators and practitioners to better manage wastewater discharges and

485    adapt to new UV technologies.

**Acknowledgments**

490

**References**

492    1.       Prüss A, Kay D, Fewtrell L, Bartram J. Estimating the burden of disease from water, sanitation,
493    and hygiene at a global level. Environ Health Perspect. 2002;110(5):537-42.
494    2.       Ashbolt NJ. Microbial Contamination of Drinking Water and Human Health from Community
495    Water Systems. Curr Environ Health Rep. 2015;2(1):95-106.
496    3.       Hijnen WAM, Beerendonk EF, Medema GJ. Inactivation credit of UV radiation for viruses,
497    bacteria and protozoan (oo)cysts in water: A review. Water Res. 2006;40(1):3-22.
498    4.       Rodriguez RA, Bounty S, Beck S, Chan C, McGuire C, Linden KG. Photoreactivation of
499    bacteriophages after UV disinfection: Role of genome structure and impacts of UV source. Water Res.
500    2014;55:143-9.
501    5.       Würtele MA, Kolbe T, Lipsz M, Külberg A, Weyers M, Kneissl M, et al. Application of GaN-based
502    ultraviolet-C light emitting diodes – UV LEDs – for water disinfection. Water Res. 2011;45(3):1481-9.
503    6.       Bolton James R, Cotton Christine A. Ultraviolet Disinfection Handbook. 1st ed. Denver:
504    American Water Works Association (AWWA); 2011.
505    7.       Vilhunen S, Särkkä H, Sillanpää M. Ultraviolet light-emitting diodes in water disinfection.
506    Environmental Science and Pollution Research. 2009;16(4):439-42.
507    8.       Banas MA, Crawford MH, Ruby DS, Ross MP, Nelson JS, Allerman AA, et al. Final LDRD report:
508    ultraviolet water purification systems for rural environments and mobile applications. Sandia National
509    Laboratories; 2005.
510    9.       Hu X, Deng J, Zhang JP, Lunev A, Bilenko Y, Katona T, et al. Deep ultraviolet light-emitting
511    diodes. physica status solidi (a). 2006;203(7):1815-8.
512    10.      Song K, Mohseni M, Taghipour F. Application of ultraviolet light-emitting diodes (UV-LEDs) for
513    water disinfection: A review. Water Res. 2016;94:341-9.
514    11.      Harris TR, Pagan JG, Batoni P. Optical and Fluidic Co-Design of a UV-LED Water Disinfection
515    Chamber. ECS Transactions. 2013;45(17):11-8.

516  12.      Standard AN. Ultraviolet Microbiological Water Treatment Systems. NSF/ANSI 55. USA: NSF
517  International; 2019.
518  13.      Chatterjee N, Walker GC. Mechanisms of DNA damage, repair, and mutagenesis.
519  Environmental and Molecular Mutagenesis. 2017;58(5):235-63.
520  14.      Sinha RP, Häder D-P. UV-induced DNA damage and repair: a review. Photochemical &
521  Photobiological Sciences. 2002;1(4):225-36.
522  15.      Jungfer C, Schwartz T, Obst U. UV-induced dark repair mechanisms in bacteria associated with
523  drinking water. Water Res. 2007;41(1):188-96.
524  16.      Smith KC, Wang T-CV, Sharma RC. recA-Dependent DNA repair in UV-irradiated Escherichia
525  coli. Journal of Photochemistry and Photobiology B: Biology. 1987;1(1):1-11.
526  17.      Setlow RB, Carrier WL. The Disappearance of Thymine Dimers from DNA: An Error-Correcting
527  Mechanism. Proc Natl Acad Sci U S A. 1964;51(2):226-31.
528  18.      Jagger J. Photoreactivation. Bacteriol Rev. 1958;22(2):99-142.
529  19.      Sancar A. Structure and Function of DNA Photolyase and Cryptochrome Blue-Light
530  Photoreceptors. Chemical Reviews. 2003;103(6):2203-38.
531  20.      Marizcurrena JJ, Martínez-López W, Ma H, Lamparter T, Castro-Sowinski S. A highly efficient
532  and cost-effective recombinant production of a bacterial photolyase from the Antarctic isolate
533  Hymenobacter sp. UV11. Extremophiles. 2019;23(1):49-57.
534  21.      Gaston KJ, Bennie J, Davies TW, Hopkins J. The ecological impacts of nighttime light pollution:
535  a mechanistic appraisal. Biological Reviews of the Cambridge Philosophical Society. 2013;88(4):912-
536  27.
537  22.      Song K, Taghipour F, Mohseni M. Microorganisms inactivation by wavelength combinations of
538  ultraviolet light-emitting diodes (UV-LEDs). Science of The Total Environment. 2019;665:1103-10.
539  23.      Kashimada K, Kamiko N, Yamamoto K, Ohgaki S. Assessment of photoreactivation following
540  ultraviolet light disinfection. Water Science and Technology. 1996;33(10):261-9.
541  24.      Tosa K, Hirata T. Photoreactivation of enterohemorrhagic Escherichia coli following UV
542  disinfection. Water Res. 1999;33(2):361-6.
543  25.      Beggs CB. A quantitative method for evaluating the photoreactivation of ultraviolet damaged
544  microorganisms. Photochemical & Photobiological Sciences. 2002;1(6):431-7.
545  26.      Sahan M. The measurements of the global solar radiation and solar ultraviolet radiation during
546  2018 year. AIP Conference Proceedings. 2019;2178(1):030016.
547  27.      Velez-Colmenares JJ, Acevedo A, Salcedo I, Nebot E. New kinetic model for predicting the
548  photoreactivation of bacteria with sunlight. J Photochem Photobiol B-Biol. 2012;117:278-85.
549  28.      Chan H-L, Gaffney PR, Waterfield MD, Anderle H, Peter Matthiessen H, Schwarz H-P, et al.
550  Proteomic analysis of UVC irradiation-induced damage of plasma proteins: Serum amyloid P
551  component as a major target of photolysis. FEBS Letters. 2006;580(13):3229-36.
552  29.      Nelson KL, Boehm AB, Davies-Colley RJ, Dodd MC, Kohn T, Linden KG, et al. Sunlight-mediated
553  inactivation of health-relevant microorganisms in water: a review of mechanisms and modeling
554  approaches. Environmental Science: Processes & Impacts. 2018;20(8):1089-122.
555  30.      Li G-Q, Wang W-L, Huo Z-Y, Lu Y, Hu H-Y. Comparison of UV-LED and low pressure UV for water
556  disinfection: Photoreactivation and dark repair of Escherichia coli. Water Res. 2017;126:134-43.
557  31.      Thiagarajan V, Byrdin M, Eker APM, Müller P, Brettel K. Kinetics of cyclobutane thymine dimer
558  splitting by DNA photolyase directly monitored in the UV. Proc Natl Acad Sci U S A. 2011;108(23):9402-
559  7.
560  32.      Douki T, Sage E. Dewar valence isomers, the third type of environmentally relevant DNA
561  photoproducts induced by solar radiation. Photochemical & Photobiological Sciences. 2016;15(1):24-
562  30.
563  33.      Foukal P. Solar astrophysics. . 2nd ed: Wiley-VCH; 2004.
564  34.      Kollu K, Ormeci B. Regrowth Potential of Bacteria after Ultraviolet Disinfection in the Absence
565  of Light and Dark Repair. Journal of Environmental Engineering. 2015;141(3).
566  35.      Thomas JD. The role of dissolved organic matter, particularly free amino acids and humic
567  substances, in freshwater ecosystems. Freshwater Biology. 1997;38(1):1-36.

568    36.    Nyangaresi PO, Qin Y, Chen G, Zhang B, Lu Y, Shen L. Effects of single and combined UV-LEDs
569    on inactivation and subsequent reactivation of E. coli in water disinfection. Water Res. 2018;147:331-
570    41.
571    37.    Cormier J, Janes M. A double layer plaque assay using spread plate technique for enumeration
572    of bacteriophage MS2. J Virol Methods. 2014;196:86-92.
573    38.    Bolton JR, Linden KG. Standardization of Methods for Fluence (UV Dose) Determination in
574    Bench-Scale UV Experiments. Journal of Environmental Engineering. 2003;129(3):209-15.
575    39.    Murov SL, Hug GL, Carmichael I. Handbook of photochemistry. 2nd ed., rev. and expanded. ed:
576    M. Dekker; 1993.
577    40.    Beck SE, Ryu H, Boczek LA, Cashdollar JL, Jeanis KM, Rosenblum JS, et al. Evaluating UV-C LED
578    disinfection performance and investigating potential dual-wavelength synergy. Water Res.
579    2017;109:207-16.
580    41.    Muela A, Garcia-Bringas JM, Arana I, Barcina I. Humic Materials Offer Photoprotective Effect
581    to Escherichia coli Exposed to Damaging Luminous Radiation. Microbial Ecology. 2000;40(4):336-44.
582    42.    Tikhonov VV, Yakushev AV, Zavgorodnyaya YA, Byzov BA, Demin VV. Effects of humic acids on
583    the growth of bacteria. Eurasian Soil Science. 2010;43(3):305-13.
584    43.    Bren A, Park JO, Towbin BD, Dekel E, Rabinowitz JD, Alon U. Glucose becomes one of the worst
585    carbon sources for E.coli on poor nitrogen sources due to suboptimal levels of cAMP. Sci Rep.
586    2016;6:24834-.
587    44.    Besaratinia A, Yoon JI, Schroeder C, Bradforth SE, Cockburn M, Pfeifer GP. Wavelength
588    dependence of ultraviolet radiation-induced DNA damage as determined by laser irradiation suggests
589    that cyclobutane pyrimidine dimers are the principal DNA lesions produced by terrestrial sunlight.
590    FASEB J. 2011;25(9):3079-91.
591    45.    Pousty D, Hofmann R, Gerchman Y, Mamane H. Wavelength-dependent time–dose reciprocity
592    and stress mechanism for UV-LED disinfection of Escherichia coli. Journal of Photochemistry and
593    Photobiology B: Biology. 2021;217:112129.
594    46.    Hoerter JD, Arnold AA, Kuczynska DA, Shibuya A, Ward CS, Sauer MG, et al. Effects of sublethal
595    UVA irradiation on activity levels of oxidative defense enzymes and protein oxidation in Escherichia
596    coli. Journal of Photochemistry and Photobiology B: Biology. 2005;81(3):171-80.
597    47.    Bosshard F, Riedel K, Schneider T, Geiser C, Bucheli M, Egli T. Protein oxidation and aggregation
598    in UVA-irradiated Escherichia coli cells as signs of accelerated cellular senescence. Environmental
599    Microbiology. 2010;12(11):2931-45.
600    48.    Cadet J, Sage E, Douki T. Ultraviolet radiation-mediated damage to cellular DNA. Mutation
601    Research, Fundamental and Molecular Mechanisms of Mutagenesis. 2005;571(1):3-17.
602    49.    Anesio AM, Granéli W, Aiken GR, Kieber DJ, Mopper K. Effect of Humic Substance
603    Photodegradation on Bacterial Growth and Respiration in Lake Water. Appl Environ Microbiol.
604    2005;71(10):6267-75.
605    50.    Bosshard F, Bucheli M, Meur Y, Egli T. The respiratory chain is the cell&apos;s Achilles&apos;
606    heel during UVA inactivation in Escherichia coli. Microbiology. 2010;156(7):2006-15.
607    51.    Nebot Sanz E, Salcedo Dávila I, Andrade Balao JA, Quiroga Alonso JM. Modelling of reactivation
608    after UV disinfection: Effect of UV-C dose on subsequent photoreactivation and dark repair. Water Res.
609    2007;41(14):3141-51.
610    52.    Roshan DR, Koc M, Abdallah A, Martin-Pomares L, Isaifan R, Fountoukis C. UV Index Forecasting
611    under the Influence of Desert Dust: Evaluation against Surface and Satellite-Retrieved Data.
612    Atmosphere. 2020;11(1):17.
613    53.    Berney M, Weilenmann HU, Ihssen J, Bassin C, Egli T. Specific growth rate determines the
614    sensitivity of Escherichia coli to thermal, UVA, and solar disinfection. Appl Environ Microbiol.
615    2006;72(4):2586-93.
616    54.    Probst-Rüd S, McNeill K, Ackermann M. Thiouridine residues in tRNAs are responsible for a
617    synergistic effect of UVA and UVB light in photoinactivation of Escherichia coli. Environmental
618    Microbiology. 2017;19(2):434-42.

619    55.    Song K, Mohseni M, Taghipour F. Mechanisms investigation on bacterial inactivation through
620    combinations of UV wavelengths. Water Res. 2019;163:9.
621    56.    Bohrerova Z, Linden KG. Standardizing photoreactivation: Comparison of DNA photorepair rate
622    in Escherichia coli using four different fluorescent lamps. Water Res. 2007;41(12):2832-8.
623    57.    Gayán E, Condón S, Álvarez I. Biological Aspects in Food Preservation by Ultraviolet Light: a
624    Review. Food and Bioprocess Technology. 2014;7(1):1-20.
625    58.    Jagger J. Near-UV radiation effects on microorganisms. Photochemistry and Photobiology.
626    1981;34(6):761-8.
627    59.    Hallmich C, Gehr R. Effect of pre- and post-UV disinfection conditions on photoreactivation of
628    fecal coliforms in wastewater effluents. Water Res. 2010;44(9):2885-93.
629